ured position should be shifted by this amount toward the larger of the two outer derivative peaks.

Figure 9 of Ref. 28 shows that for a dispersion-type crossing signal ($\epsilon \ll 1$) the two outer derivative peaks are shifted from their positions for $\epsilon=0$ by an amount $-\epsilon$, while the central derivative peak is shifted by $-\frac{1}{3}\epsilon$. Differentiation of Eq. (8) shows that the zero-derivative points of a dispersion-type crossing are also shifted (to first order in ϵ) by an amount $-\epsilon$. When derivative detection is used, the zero-derivative points can be determined much more precisely (provided a good baseline can be established) than can the positions of the outer derivative peaks. The central derivative peak position is corrected by shifting it *away* from the mean position of the two zero-derivative points by an amount equal to one half the difference between this mean and the observed central peak position.

2. For Overlap

The overlap of the signals from the different hyperfine crossings does not shift the position of H_0, the center of the Li^6 low-field crossing signal, but does shift the positions of H_1 through H_4, the zeros in the derivative of the Li^7 low-field crossing signal. The resolution of the hyperfine signals in Li^7 is large enough to allow us to calculate the correction for overlap by considering only two hyperfine signals at a time and then adding the results for all such overlapping pairs. For two overlapping Lorentzian signals, the signal is proportional to $[1+(\omega-\omega_0)^2]^{-1}+[1+(\omega+\omega_0)^2]^{-1}$, where again ω is the dimensionless ratio Δ/γ and $2\omega_0$ is the dimensionless spacing of the two hyperfine crossings. Setting the derivative of this expression equal to zero yields, in addition to the obvious root at $\omega=0$,

$$\omega^2=2\omega_0(\omega_0^2+1)^{1/2}-(\omega_0^2+1).$$

The differences between the roots of this equation and $\omega=\pm\omega_0$ give the shifts of the derivative zeros arising from the overlap. If $\omega_0^2<\frac{1}{3}$, the equation has no real roots and the only zero in the derivative signal is the one at $\omega=0$. For the Li^7 low-field signal, the spacings of adjacent hyperfine crossings correspond to an ω_0 of very nearly 2.

PHYSICAL REVIEW VOLUME 153, NUMBER 1 5 JANUARY 1967

"Anticrossing" Signals in Resonance Fluorescence*

H. WIEDER† AND T. G. ECK
Physics Department, Case Institute of Technology, Cleveland, Ohio
(Received 26 August 1966)

The level-crossing technique of atomic spectroscopy utilizes the spatial interference in the scattering of resonance radiation which can occur when two Zeeman levels of an atom are brought into coincidence ("crossed") by the application of an external magnetic field. "Anticrossing" refers to the case where the two levels involved are coupled by a small static interaction. In this paper the general expression for an anticrossing signal is given and its predictions compared with signals observed in the $2\,^2P$ term of Li. It is shown that anticrossings produce signals in many experimental situations for which there would be no signal from a normal level crossing.

I. INTRODUCTION

THE two most widely used techniques for investigating the fine and hyperfine structure of excited states of atoms are those of optical-double-resonance (ODR)[1] and level-crossing.[2] In both of these techniques, signals are seen which are the result of a "coupling" between two Zeeman levels of the excited state. For ODR experiments, this coupling is accomplished by the application of a rf magnetic field having the appropriate frequency, while for a level crossing the coupling in the region of the crossing is simply an intimate part of the optical excitation process.[3] In this paper we consider the situation where two crossing levels are coupled by a small static interaction (as opposed to the time-dependent coupling of ODR). The static interaction can give rise to a signal even if the properties of the optical excitation or of the two levels are such as to prohibit the presence of a normal level-crossing signal. The word "anticrossing"[4,5] has been used to distinguish this case from a normal level crossing, because it is descriptive of the manner in which the coupled levels "repel" one another as the magnetic field is varied through the region of close approach. We discuss anticrossing signals that we have observed in the $2\,^2P$ term of Li and

* Work supported by the National Science Foundation.
† Present address: IBM T. J. Watson Research Center, Yorktown Heights, New York.
[1] J. Brossel and F. Bitter, Phys. Rev. 86, 308 (1952).
[2] F. D. Colegrove, P. A. Franken, R. R. Lewis, and R. H. Sands, Phys. Rev. Letters 3, 420 (1959).
[3] P. A. Franken, Phys. Rev. 121, 508 (1961).
[4] T. G. Eck, L. L. Foldy, and H. Wieder, Phys. Rev. Letters 10, 239 (1963).
[5] T. G. Eck, paper presented at the Zeeman Centennial conference (to be published).

indicate how such signals can be used to extend the range of precise investigations of excited atomic states.

The general expression for an anticrossing signal is given in Sec. II and then reduced to a form appropriate for discussing the signals observed in the $2\,^2P$ term of Li. Sections III and IV contain the experimental results and their comparison with the theory. Suggestions for further anticrossing experiments are given in Sec. V. The work reported here was part of a detailed investigation of the fine and hyperfine structure of the $2\,^2P$ term of Li. Most of the results of that investigation are presented in the preceding paper, hereafter referred to as BEW.

II. THEORY

A. Anticrossing Signals

The calculation of the steady-state resonance fluorescence signal associated with an anticrossing is straightforward in principle. One simply calculates the steady-state signal arising from the decay of two coupled states that are excited at uniform rates. Lamb[6] considered a closely related, but more complicated, problem in his discussion of narrow resonances in the $n=2$ state of hydrogen. His treatment was for the case where one of the states being coupled did not radiate, i.e., $\gamma=1/2\pi\tau=0$, where τ is the lifetime of the state. Recently, Series[7,8] considered fluorescence from two states coupled by a static interaction, but again only for the case of $\gamma=0$ for one of the states. He found that for this special case the steady-state signal is independent of the coupling. We have examined the more general case where both states radiate but may have different values of γ and may or may not be radiatively connected to the same initial and final states in the resonance-fluorescence process. The calculation of the steady-state signal obtained for this case is briefly outlined in Appendix A. After describing qualitatively the behavior of the levels and their associated wave functions in the region of close approach, we shall state the general result for the steady-state signal and examine certain limiting forms of it.

Figure 1 shows the behavior of two anticrossing levels when $\gamma_a=\gamma_b$. The symbols a and b refer to the levels and wave functions in the absence of coupling, and a' and b' the levels and wave functions when coupling is present. The dashed levels a and b cross ($\Delta=0$) at $H=H_0$. While the levels a' and b' never cross, they attain their distance of closest approach for this value of H. The minimum separation of the levels is simply $|2V|$, where V is the matrix element of the interaction coupling the states a and b. The energies and wave functions of a' and b' are readily obtained for any value of Δ, the frequency separation between levels a and b, by diagonalizing the energy matrix for states a and b. As H is varied through the region of H_0, the wave functions of a' and b' interchange their identities, i.e., $\psi_{a'}\approx\psi_a$ for $H\ll H_0$ and $\psi_{a'}\approx\psi_b$ for $H\gg H_0$. At $H=H_0$ the wave functions of a' and b' are 50-50 mixtures of those of a and b.

Figure 51 of Ref. 6 shows the behavior of anticrossing levels when $\gamma_a\neq\gamma_b$. This figure is for the special case where one of the γ's is equal to zero, but it and the accompanying discussion of the mixing of states are qualitatively correct for any γ_a and γ_b. There is a cusping of the levels a' and b' toward one another as H approaches H_0, the amount of this cusping being determined by the ratio of $[(\gamma_a-\gamma_b)/4]^2$ to $|V|^2$. If this ratio is equal to one, then at $H=H_0$ the levels a' and b' just touch and their wave functions are again equal mixtures of the wave functions of the levels a and b. For large values of the ratio, the levels cross and there is very little state mixing, while small values of the ratio give, of course, a behavior very nearly that for $\gamma_a=\gamma_b$.

The steady-state anticrossing signal, expressed as a function of Δ and in terms of the properties of the eigenstates a and b (which do not vary appreciably over the region of the anticrossing), is

$$
\begin{aligned}
S=&(1/\gamma_a)\sum_{[1]}[|f_a|^2|g_a|^2]+(1/\gamma_b)\sum_{[2]}[|f_b|^2|g_b|^2]\\
&+(\gamma_a\gamma_b/\bar\gamma D)\sum_{[3]}[f_af_b^*g_ag_b^*+f_a^*f_bg_a^*g_b]-(i\gamma_a\gamma_b\Delta/\bar\gamma^2D)\sum_{[4]}[f_af_b^*g_ag_b^*-f_a^*f_bg_a^*g_b]\\
&-(2|V|^2\gamma_a\gamma_b/\bar\gamma D)\sum_{[5]}[fg]+(2/\bar\gamma D)\sum_{[6]}[(V^*f_af_b^*+Vf_a^*f_b)(Vg_ag_b^*+V^*g_a^*g_b)]\\
&+(\Delta\gamma_a\gamma_b/\bar\gamma^2D)\sum_{[7]}[f(Vg_ag_b^*+V^*g_a^*g_b)+g(V^*f_af_b^*+Vf_a^*f_b)]\\
&+(i\gamma_a\gamma_b/\bar\gamma D)\sum_{[8]}[f(Vg_ag_b^*-V^*g_a^*g_b)+g(V^*f_af_b^*-Vf_a^*f_b)], \qquad (1)
\end{aligned}
$$

where $D=\gamma_a\gamma_b+|2V|^2+(\gamma_a\gamma_b/\bar\gamma^2)\Delta^2$ is the resonance denominator,

$$\bar\gamma=\tfrac{1}{2}(\gamma_a+\gamma_b),\quad f=(|f_a|^2/\gamma_a)-(|f_b|^2/\gamma_b),$$
$$g=(|g_a|^2/\gamma_a)-(|g_b|^2/\gamma_b),$$

and V is the matrix element of the static interaction which couples states a and b. The symbol f_a is an abbreviated notation for $f_{am}\equiv\langle a|\mathbf{f}\cdot\mathbf{r}|m\rangle$, the electric dipole matrix element for excitation to state a from state m. Similarly, $g_a\equiv g_{m'a}\equiv\langle m'|\mathbf{g}\cdot\mathbf{r}|a\rangle$ is the matrix element for spontaneous decay from state a to state m'. The starring of a quantity indicates its complex conjugate. The symbol $\sum$ before a set of brackets means that

[6] W. E. Lamb, Jr., Phys. Rev. 85, 259 (1952). Sections 68 through 72 of this paper contain the pertinent discussion.
[7] G. W. Series, Phys. Rev. Letters 11, 13 (1963).
[8] G. W. Series, Phys. Rev. 136, A684 (1964).

the quantity within the brackets is to be summed over all the relevant levels m of the initial state, and m' of the final state in the resonance-fluorescence process. All factors having to do with the intensity and spectral distribution of the resonance lamp, the spectral sensitivity of the detector, polarizations of incident and scattered light, experimental geometry, etc., are assumed to be contained in the matrix elements.

The first two terms of Eq. (1) give the nonresonant background scattering from the states a and b, while the third and fourth terms taken together are the normal level-crossing signal modified by the presence of $|2V|^2$ in the resonance denominator and written in the form appropriate for γ_a not necessarily equal to γ_b. The variation of the background signal over the region of the anticrossing is usually negligible unless the anticrossing is quite broad, either because of a large γ_a, γ_b, or V or because $\partial\Delta/\partial H$ is small (levels a and b having nearly the same slope). The observation of the level-crossing part of the signal requires "coherence" in both the excitation and detection parts of the experiment in the sense that f_{am} and f_{bm} must both be nonzero for at least one m and $g_{m'a}$ and $g_{m'b}$ both nonzero for at least one m'. This is the familiar criterion for a level-crossing signal and means that the optical excitation must excite atoms to a and b from the *same* one or more levels of the initial state and that the detector must observe transitions from a and b to the *same* one or more levels of the final state.

Term 5 of Eq. (1), which will be the important one in most anticrossing experiments, is the only "pure" anticrossing part of the signal. It vanishes for $V=0$ and does not require coherence in either the excitation or detection parts of the experiment. In fact, it is a maximum when only one of the states a or b is excited by the incident light and re-emitted light from only one of these states is detected. Furthermore, if $\gamma_a=\gamma_b$, term 5 vanishes when a and b are populated equally ($\sum|f_a|^2=\sum|f_b|^2$) or when the detection fails to discriminate between the radiations from these states ($\sum|g_a|^2=\sum|g_b|^2$). Series[7] has pointed out the very close kinship of term 5 and an ODR signal. It can be taken as a good rule of thumb that in those experimental situations where one can see an ODR signal, it should also be possible to observe a signal associated with term 5, provided that one can obtain the close approach of two coupled levels. The last three terms of Eq. (1) are mixed crossing and anticrossing terms, requiring both $V\neq 0$ and coherence in one or both of the two steps in the resonance fluorescence process. Term 6 requires coherence in both steps, and terms 7 and 8 require coherence in at least one.

To conclude our discussion of Eq. (1), we note three limiting forms of it. When $V=0$, the last four terms vanish and we are left with the nonresonant background plus the normal level-crossing signal. When γ_a or $\gamma_b=0$, all terms vanish except the second or first. This is apparent from the fact that $\gamma_a=0$ implies that f_{am} and $g_{m'a}$ are zero for all m and m', and similarly for $\gamma_b=0$.

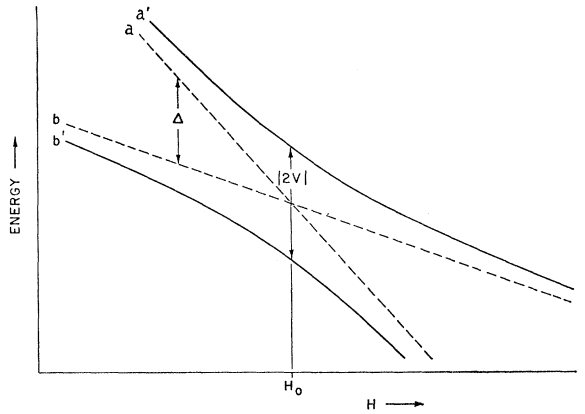

FIG. 1. The anticrossing of two energy levels for the case where both states have the same lifetime. The dashed levels show the crossing that would occur if there were no coupling between the states ($V=0$).

This absence of any crossing or anticrossing signal when one of the two states involved does not radiate agrees with Series's[7,8] analysis and the more formal treatment by Lassila.[9] Finally, if coherence is absent in both the excitation and detection steps of the resonance-fluorescence process, we are left with only the nonresonant background (terms 1 and 2) and the pure anticrossing signal (term 5).

B. High-Field Fine-Structure Crossing in the $2\,^2P$ Term of Li

Figure 1 of the preceding paper (BEW) shows that the $J=\frac{3}{2}$, $m_J=-\frac{3}{2}$ and $J=\frac{1}{2}$, $m_J=-\frac{1}{2}$ fine structure levels of a ^2P term cross at a field H_H, which for the $2\,^2P$ term of Li is equal to approximately 4800 G. We refer to this crossing as the high-field crossing to distinguish it from the crossing of the $\frac{3}{2}$, $-\frac{3}{2}$ and $\frac{1}{2}$, $\frac{1}{2}$ levels at the lower field H_L. The eight hyperfine structure levels involved in the high-field crossing in the $2\,^2P$ term of Li^7 are shown in Fig. 2. The static perturbation which couples the levels and causes them to anticross is provided in this case by the magnetic hyperfine interaction. Coupling occurs between pairs of levels having the same value of $m_F=m_J+m_I$, but different values of m_I. In Fig. 2 the levels obtained by neglecting this coupling are labeled by their m_I quantum numbers at the left of the figure, while the actual levels are labeled by their m_F quantum numbers at the right of the figure. The three squares locate the centers of the three anticrossings of the pairs of levels with $m_F=-2$, -1, 0, and the circles show the positions of the four level crossings which would be observable if the coupling were not present. Though the level-crossing signal is still observable, it is distorted by the shifts in the positions of the crossings (the $m_I=\frac{1}{2}$ and $-\frac{1}{2}$ crossings are eliminated as identifiable points and the $\frac{3}{2}$ and $-\frac{3}{2}$ crossings shifted to the regions indicated by the arrows in Fig. 2) and by the fact that the wave functions of six of the eight states are changing

[9] K. E. Lassila, Phys. Rev. **135**, A1218 (1964).

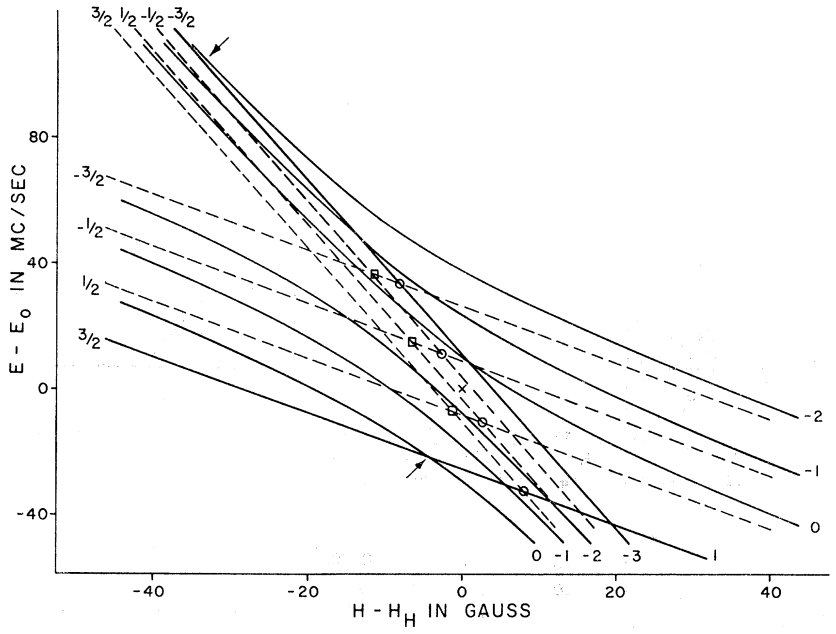

FIG. 2. The eight hyperfine levels involved in the high-field fine-structure crossing in the $2\ ^2P$ term of Li^7. To show more clearly the details of the crossing, the spacing of the four m_I levels with $m_J=-\frac{3}{2}$ has been increased by a factor of approximately $2\frac{1}{2}$. The spacing of the m_I levels with $m_J=-\frac{1}{2}$ is correct as shown.

rapidly over the region of the crossing. Thus, it is difficult to extract fine- and hyperfine-structure information from the crossing part of the high-field crossing signal. Fortunately, the anticrossing part of the signal is not distorted and can be easily analyzed, provided that it is possible to eliminate the crossing signal and observe the pure anticrossing signal. For Li^6 with $I=1$, one obtains the same effect as that shown in Fig. 2, except that there are two anticrossings and three crossings. The distortion of the crossing signal in Li^6 is less than that in Li^7, but still present.

Since each pair of levels that are mixed in each of the three anticrossings of Fig. 2 have different values of m_I, they cannot both be excited from the same level of the ground state and cannot decay to the same ground-state level. Using this property plus $\gamma_a=\gamma_b=\gamma$ in Eq. (1), we obtain for the anticrossing part of the high-field crossing signal [omitting the nonresonant background terms in Eq. (1)]

$$S_{\text{anti}}=-[2|V|^2/\gamma(\gamma^2+|2V|^2+\Delta^2)] \times[\textstyle\sum_m|f_{am}|^2-\sum_n|f_{bn}|^2] \times[\textstyle\sum_m|g_{ma}|^2-\sum_n|g_{nb}|^2], \quad (2)$$

where the summations over m and n are nonoverlapping. The total anticrossing signal is a superposition of three such signals (with strong overlap) for Li^7 and two for Li^6. It should be noted that the signal given by Eq. (2) has a Lorentzian line shape for any experimental geometry. There is not the mixture of Lorentzian and dispersion-type line shapes which occurs in level-crossing experiments for all but special angles of scattering. The dependence of the anticrossing signal on the polarizations of the incident and detected light can be readily determined by evaluating the matrix elements f_{am}, f_{bn}, etc., using the wave functions of Appendix A of BEW and the properties of a T vector given on page 63 of Condon and Shortley.[10] For our experimental geometry, where the propagation vectors of the incident and detected light were perpendicular to **H** and to one another, we find

$$S_{\text{anti}}\propto(3\cos^2\theta_1-1)(3\cos^2\theta_2-1), \quad (3)$$

where θ_1 and θ_2 are the angles between **H** and the planes of polarization of the incident and detected light. Significant discrepancies were found between the experimental results and the predictions of Eq. (3) for reasons discussed in Sec. IV.

The form which the crossing part of the high-field crossing signal would take if there were no coupling of states is given by Eq. (7) of BEW. Evaluating the matrix elements in the manner indicated above, we find that for our experimental geometry the undistorted crossing signal would have a dispersion-type line shape and a dependence on Polaroid orientations given by

$$S_{\text{cross}}\propto\sin(2\theta_1)\sin(2\theta_2). \quad (4)$$

The coupling distorts the line shape, but does not alter Eq. (4). Equations (3) and (4) together predict that a pure anticrossing signal can be obtained for θ_1 or $\theta_2=0°$ or 90°, and a pure crossing signal for θ_1 or $\theta_2=\cos^{-1}\frac{1}{3}\sqrt{3}$. If θ_1 or θ_2 is set at $\cos^{-1}\frac{1}{3}\sqrt{3}$ and the other Polaroid oriented either parallel or perpendicular to **H**, both signals should vanish. This analysis clarifies the reasons for the experimental procedures which were chosen to obtain anticrossing information, and which are described in detail in Sec. III.

The matrix element V responsible for the anti-

[10] E. U. Condon and G. H. Shortley, *The Theory of Atomic Spectra* (Cambridge University Press, Cambridge, England, 1953).

crossing signal is the magnetic dipole matrix element $\langle \frac{3}{2}, -\frac{3}{2}, m_I+1 | \mathcal{H}_D | \frac{1}{2}, -\frac{1}{2}, m_I \rangle$ given in Appendix A of BEW. In the vicinity of the high-field crossing

$$V=(\tfrac{1}{6}\sqrt{3})[(I-m_I)(I+m_I+1)]^{1/2}[(6/5)\alpha\langle 1/r^3\rangle-\xi]. \quad (5)$$

This can be evaluated using the values of $\alpha\langle 1/r^3\rangle$ and ξ determined in BEW. The value of V can also be obtained from the width of any one of the overlapping components of the anticrossing signal (two for Li^6 and three for Li^7) and a knowledge of γ. Setting the second derivative of Eq. (2) with respect to Δ equal to zero yields

$$\delta_P=(2/\sqrt{3})(\gamma^2+|2V|^2)^{1/2}, \quad (6)$$

where δ_P is the peak-to-peak derivative width of a single component of the anticrossing signal. Before Eq. (6) can be used to find $|V|$, some means must be found to deduce the width of a single component signal from the observed width of the total signal. The discussion of Appendix B shows how to obtain this information for equally spaced components, provided the spacing of the centers of the component signals is known. This spacing can be obtained with sufficient precision from the difference between the $\langle \frac{3}{2}, -\frac{3}{2}, m_I | \mathcal{H}_D | \frac{3}{2}, -\frac{3}{2}, m_I \rangle$ and $\langle \frac{1}{2}, -\frac{1}{2}, m_I | \mathcal{H}_D | \frac{1}{2}, -\frac{1}{2}, m_I \rangle$ matrix elements of Appendix A of BEW.

$$\text{Spacing}=[(4/15)\alpha\langle 1/r^3\rangle-\tfrac{1}{3}\xi]. \quad (7)$$

Finally, we wish to be able to infer the field H_H at which the center of the high-field crossing signal would occur if there were no coupling (the point marked with an × in Fig. 2). To find the amount by which the center of the anticrossing signal is shifted down in field from H_H, we consult Fig. 2, the corresponding diagram for Li^6, and Eq. (3) of BEW. The quadrupole interaction $\mathcal{H}_Q$ contributes a negligible amount to this shift. Again using the appropriate matrix elements of $\mathcal{H}_D$ given in Appendix A of BEW and analyzing the geometry of Fig. 2, we find for Li^7

$$\text{Shift}=[g_I\mu_0 H+(14/15)\alpha\langle 1/r^3\rangle+\tfrac{1}{3}\xi](\partial\Delta/\partial H)^{-1}. \quad (8)$$

This expression for the shift also holds for Li^6. We find H_H by adding the field interval given by Eq. (8) to the field corresponding to the center of the anticrossing signal. To the precision of the data, it is immaterial whether one takes H in $g_I\mu_0 H$ to be H_H or the center of the anticrossing.

III. EXPERIMENTAL PROCEDURE

A description of the apparatus and most of the details of the experimental procedure are given in Secs. III and IV of BEW. Only two additional points need to be discussed.

To separate the crossing and anticrossing parts of the high-field crossing signal and to test the predictions of Eqs. (3) and (4), it is necessary to be able to determine the orientations of the Polaroids with high precision. The Polaroids were mounted so that their orientations could be reproducibly set and read to within approximately one-half degree with respect to fixed fiducial marks on their mountings. The orientation of one of the Polaroids corresponding to its plane of polarization parallel to **H** was found by setting this Polaroid approximately parallel to **H** (using light reflected at grazing incidence from a glass plate) and rotating the second Polaroid to the orientation for which the anticrossing signal vanished. This latter orientation was quite easy to locate, since the anticrossing signal, which is changing more rapidly with angle than the residual crossing signal, changes sign at this orientation. With the second Polaroid set at this orientation, the first was aligned parallel to **H** by setting it to eliminate the crossing signal. The orientation of the second Polaroid was then calibrated with respect to its fiducial mark by interchanging the roles of the two Polaroids and repeating the above procedure.

As discussed in Sec. IV of BEW, the centers of the low-field crossing signals were found by manually adjusting H to values that gave sharp nulls in the 40 cps signal from the tuned amplifier of the lock-in detector. This technique was not used to find the center of the crossing part of the high-field crossing signal, since the derivative of a dispersion-type line shape is not zero at its center, but a maximum, and is considerably more difficult to locate accurately. It was also found to be inapplicable to the anticrossing signal, since at the center of the anticrossing, as determined from pairs of recorder traces, there was still an appreciable 40 cps signal from the tuned amplifier. This residual 40 cps signal arises from magnetic tuning of the Zeeman levels of the scatterer over the spectral profile of the lamp [see Sec. IV of BEW]. It is not surprising that this background signal is much larger for the anticrossing signal than for the low-field crossing signal, since about 10 times larger amplitudes of magnetic-field modulation are required for a comparable signal-to-noise ratio, and since at the higher field the Zeeman levels are shifted, on the average, further from the center of the lamp profile. The data discussed in the following section were all obtained from pairs of recorder traces (one sweeping up in field strength and the other down) calibrated with proton frequency markers.

IV. RESULTS AND ANALYSIS

Typical recorder traces of the derivatives of the anticrossing and crossing parts of the high-field crossing signal in the $2\,^2P$ term of Li are shown in Figs. 3–6. The anticrossing traces (Figs. 3 and 4) were taken with both Polaroids aligned parallel to **H**, and the crossing traces with both θ_1 and θ_2 set at the angles for which the anticrossing signal vanishes as determined by the procedure outlined in Sec. III. While the crossing signal in Li^6 (Fig. 5) is only slightly distorted from the shape expected for the derivative of a dispersion-type line shape,

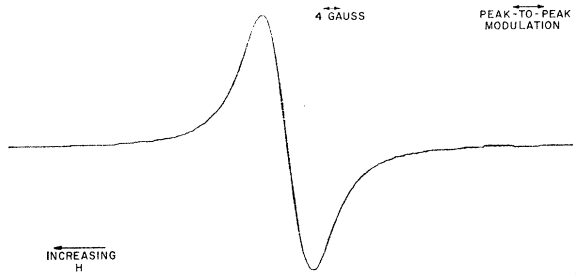

FIG. 3. Recorder trace of the derivative of the anticrossing signal in the $2\,^2P$ term of Li^6.

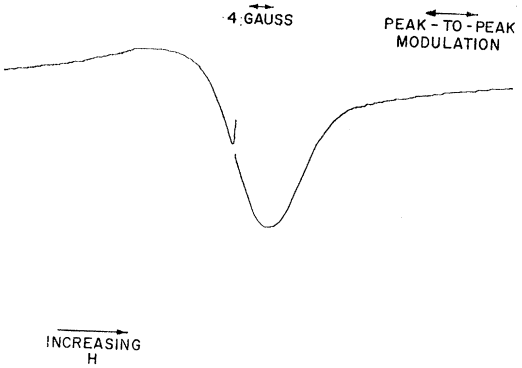

FIG. 6. Recorder trace of the derivative of the high-field crossing signal in the $2\,^2P$ term of Li^7. The spike in the trace is a field marker.

the distortion of the Li^7 crossing signal (Fig. 6) is very pronounced. This greater distortion of the Li^7 signal is to be expected, since the magnetic hyperfine interaction in Li^7 exceeds that in Li^6 by a factor of approximately 8/3. In going from Li^6 to Li^7, both the coupling matrix element V and the range of H over which the crossings occur are scaled by roughly this factor.

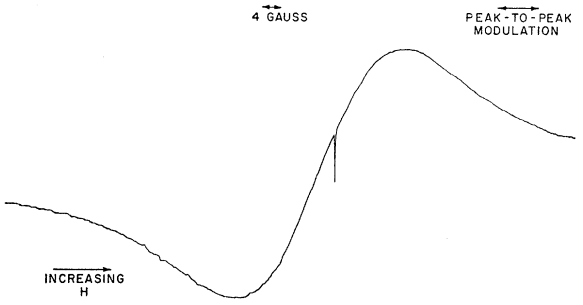

FIG. 4. Recorder trace of the derivative of the anticrossing signal in the $2\,^2P$ term of Li^7. The spike in the trace is a field marker.

Table I compares the experimentally observed dependence of the strength of the anticrossing signal on Polaroid orientation with that predicted by Eq. (3). θ_{V1} and θ_{V2} are the Polaroid orientations for which the anticrossing signal vanishes, and the plus and minus signs denote the relative phase of the signal. Large discrepancies between the experimental results and the predictions of Eq. (3) occur for those combinations of Polaroid settings which admit to the scattering chamber the component of the incident light which is polarized perpendicular to **H**. Also, while the experimental and predicted values of θ_{V2} are in good agreement, the discrepancy between these values of θ_{V1} is much too large to be explained by the uncertainty in the experimental value of this angle. The most plausible explanation for these discrepancies is that one or more of the transitions from the ground state to the anticrossing levels lie outside the spectral distribution of our lamp, since the lamp is located in a fringe field of less than 10 G. For $H=H_H$, the frequencies of the transitions from the $J=\frac{1}{2}$, $m_J=\frac{1}{2}$, m_I levels of the ground state to the $\frac{1}{2}$, $-\frac{1}{2}$, m_I levels of the $2\,^2P$ term are reduced by about 10^4 Mc/sec from their values for $H\approx 0$. Thus, it is quite likely that these transitions are not induced by the lamp. Recalculating the anticrossing signal with the omission of the excitation matrix elements corresponding to these transitions yields

$$S_{\text{anti}} \propto [\tfrac{7}{2}\cos^2\theta_1 - \tfrac{3}{2}][3\cos^2\theta_2 - 1]. \qquad (9)$$

The last column of Table I gives the relative signal strengths predicted by Eq. (9). They are definitely in

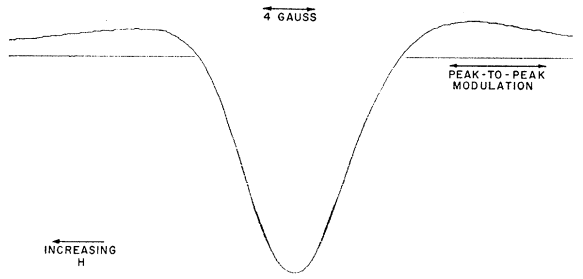

FIG. 5. Recorder trace of the derivative of the high-field crossing signal in the $2\,^2P$ term of Li^6.

TABLE I. Dependence of anticrossing signal on Polaroid orientations.

		Strength relative to $\theta_1=\theta_2=0°$ signal		
θ_1	θ_2	Expt.	Eq. (3)	Eq. (9)
0°	0°	+1.00	+1.00	+1.00
0°	90°	−0.55	−0.50	−0.50
90°	0°	−0.83	−0.50	−0.75
90°	90°	+0.43	+0.25	+0.375
0°	none[a]	+0.64 (+0.48)[b]	+0.50	+0.50
none[a]	0°	+0.19 (+0.14)[b]	+0.50	+0.25
none[a]	none[a]	+0.09 (+0.05)[b]	+0.25	+0.125
	θ_{V1}	48°	55°	49°
	θ_{V2}	55°	55°	55°

[a] Polaroid removed.
[b] Renormalized to account for the effect of Polaroid absorption.

better agreement with the experimental results than the predictions of Eq. (3). Thus, we conclude that the transitions from the $\frac{1}{2}$, $\frac{1}{2}$, m_I levels of the ground state to the $\frac{1}{2}$, $-\frac{1}{2}$, m_I levels of the $2\,^2P$ term are indeed only weakly excited by our lamp.

A few words are in order regarding apparent internal inconsistencies in the experimental results given in Table I. For example, the relative signal of $+0.64$ for $\theta_1=0°$ and no Polaroid in front of the detector does not equal, as it should, the value of $+0.45$ given by the sum of the signals for $\theta_1=0°$ and $\theta_2=0°$ and 90°. The difference between these two signals is satisfactorily explained by the fact that at 6708 Å, HN-32 Polaroid sheet transmits only about 75% of the light polarized parallel to the axis of the Polaroid (and a negligible fraction of the light polarized perpendicular to the axis). The entries in parentheses in column 3 of Table I are the experimental signals renormalized to account for the effect of Polaroid absorption.

The peak-to-peak derivative widths of the anticrossing signals in Li^6 and Li^7 were determined from recorder traces of these signals, 10 in the case of Li^6 and four in the case of Li^7. These widths, corrected for modulation broadening[11] and converted to frequency units using 1.866 Mc/sec G for $\partial\Delta/\partial H$ and 4.2577 kc/sec G for the conversion factor between proton resonance frequency and magnitude field strength, are

$$Li^6: \quad 19.67\pm0.20 \text{ Mc/sec},$$
$$Li^7: \quad 66.66\pm0.67 \text{ Mc/sec},$$

where the uncertainties of 1% are about two times the standard deviations and represent our 80% confidence limits. The spacings between the hyperfine components of the anticrossing signals can be calculated from Eq. (7) using for Li^7 the values of $\alpha\langle 1/r^3\rangle$ and ξ found in BEW and for Li^6 these values scaled by $g_I(Li^6)/g_I(Li^7)=0.3786$. When the spacings and measured derivative widths are used in the expressions developed in Appendix B, we find for the derivative width of a single component of the anticrossing signal

$$Li^6: \quad 18.22\pm0.20 \text{ Mc/sec},$$
$$Li^7: \quad 58.71\pm0.67 \text{ Mc/sec}.$$

Substituting these results into Eq. (6) and using for $\gamma=1/2\pi\tau$ the value determined by the τ given in BEW, we obtain for the matrix element V responsible for the anticrossing signal

$$V(Li^6)= 7.33\pm0.08 \text{ Mc/sec},$$
$$V(Li^7)=25.25\pm0.30 \text{ Mc/sec}.$$

Equation (5) can be used to calculate V directly from the hyperfine interaction constants. This gives

$$V(Li^6)= 7.36\pm0.11 \text{ Mc/sec},$$
$$V(Li^7)=25.05\pm0.37 \text{ Mc/sec},$$

where for Li^7 the value of V for the central hyperfine component of the anticrossing signal is larger than that for the other two, and we have taken the average of the three values 23.82, 27.51, 23.82 Mc/sec. As discussed in BEW, the excellent agreement between the values of V obtained from the anticrossing signal widths and those calculated directly from the hyperfine interaction constants is quite convincing evidence for the adequacy of our theoretical treatment of the hyperfine-structure data.

The magnetic field strengths corresponding to the centers of the anticrossing signals were determined from pairs of recorder traces, five pairs for Li^6 and four for Li^7. The average of the measured field strengths, corrected for line shape distortion in the manner discussed in Appendix C1 of BEW, are

$$Li^6: \quad 20366.2\pm0.7 \text{ kc/sec};$$
$$Li^7: \quad 20350.8\pm4.0 \text{ kc/sec},$$

where again the uncertainties represent 80% confidence limits. The large uncertainty in the position of the Li^7 anticrossing is a reflection primarily of the uncertainty in the baseline of the recorder traces of this signal. A large amplitude of modulation of the magnetic field was required to obtain a good signal-to-noise ratio for this broad signal, with the result that there was an appreciable slope to the baseline even far from the crossing. This uncertainty in the baseline caused not only an uncertainty in the location of the center of the anticrossing signal, but also an uncertainty in the correction for line shape distortion. Since for a given fractional distortion the correction is proportional to the signal width, a small uncertainty in the distortion can cause an appreciable uncertainty in the position of the center of a broad signal.

When the field intervals calculated from Eq. (8) are added to the field strengths of the centers of the anticrossings, we find for H_H, the center of the high-field fine structure crossing,

$$H_H(Li^6)=20374.8\pm0.8 \text{ kc/sec},$$
$$H_H(Li^7)=20373.4\pm4.0 \text{ kc/sec}.$$

The quadrupole and off-diagonal dipole matrix elements of the hyperfine interaction produce small shifts in the positions of the hyperfine levels, but these change the values of H_H by amounts that are negligible compared to the experimental uncertainties in these field strengths. In BEW we determined for Li^6 and Li^7 the value of H_L, the position of the low-field fine structure crossing. Combining these results with the above values of H_H, we obtain for the ratio of H_H to H_L

$$Li^6: \quad 1.49928\pm0.00006,$$
$$Li^7: \quad 1.49912\pm0.00030.$$

Equation (2) of BEW predicts that this ratio should be equal to $(g_S+g_L)/g_S$. Taking $g_S=2.00232$ and

[11] H. Wahlquist, J. Chem. Phys. 35, 1708 (1961).

$g_L = 1 - m/M$, where m is the electron mass and M is the nuclear mass, we find that the theoretical ratio is 1.49938 for both Li^6 and Li^7. The small discrepancy between the theoretical ratio and the experimental ratio for Li^6 arises most likely from our neglect of relativistic and diamagnetic corrections[12] to g_L.

Finally, the field strength corresponding to the central derivative peak of the level-crossing part of the high-field crossing signal was determined for both Li^6 and Li^7 using five pairs of recorder traces for Li^6 and four for Li^7. The results,

$$Li^6: \quad 20374 \pm 1 \text{ kc/sec},$$
$$Li^7: \quad 20368 \pm 1 \text{ kc/sec},$$

were not corrected for instrumental distortion of the line shape, since such distortion cannot be separated out from that caused by the state coupling responsible for the anticrossing signal. These peak positions are quite close to the values of H_H determined above, which for Li^7 is somewhat surprising in view of the large distortion of the Li^7 crossing signal.

V. DISCUSSION

Although in the preceding sections of this paper we have been concerned with resonance-fluorescence signals in atomic systems, the reader should not deduce from this that anticrossing signals are restricted to resonance-fluorescence experiments or can only be seen in experiments involving free atoms. Whenever a physical system possesses sharp energy levels that can be tuned through one another by the application of an external field and a static coupling exists between these levels, an anticrossing signal should be observable. The work of van der Ziel and Bloembergen[13] shows how anticrossing signals can be used to investigate the crystalline fields in solids via their perturbations of the sharp energy levels of substituted ions. Robiscoe's[14] measurement of the Lamb shift in the $n=2$ state of hydrogen can be viewed as an anticrossing experiment where the state coupling is produced by the applied electric field and the anticrossing signal arises from the increased quenching of the $2S$ state in the region of the crossing.

To illustrate the types of anticrossing experiments which can be used to investigate excited states of atoms, we shall discuss briefly an experiment now underway in our laboratory, an investigation of the fine and hyperfine structure of the $3\,^2D$ term of Li. The energy levels of the $3\,^2D$ term of Li can be populated by radiative decay following optical excitation to the $4\,^2P$ term or can be excited directly from the ground state by electron bombardment. In the case of optical excitation, a normal level-crossing experiment is ruled out by the loss of angular correlation due to the added step in the excitation process. For the observation of a level-crossing signal with electron bombardment excitation, the electron beam must have an appreciable component of velocity in a unique direction perpendicular to the magnetic field.[15] This limits the investigation to the zero-field crossing signal (Hanle effect), which gives no information about fine or hyperfine structure splittings, or requires replacement of the electron beam by a high-energy beam of ions. Observation of an anticrossing signal requires only that the states involved in the anticrossing be populated unequally and the detection be such as to discriminate between the radiations from these states. There are naturally occurring anticrossings (caused by off-diagonal matrix elements of the magnetic hyperfine interaction) associated with two of the fine structure crossings in the $3\,^2D$ term of Li, and there are three more fine structure crossings which can be converted into anticrossings by the application of an electric field perpendicular to the magnetic field. The results of Budick *et al.*,[16] indicate that electric field strengths of 10000 V/cm should be sufficient to produce appreciable anticrossing signals for these three crossings. All five of the anticrossings should produce easily detectable changes in the spatial distribution and polarization of the 6103-Å transition from the $3\,^2D$ to the $2\,^2P$ term of lithium.

Series[8] implies that for the anticrossing of two levels of opposite parity all of the terms in Eq. (1) vanish except the first two, the nonresonant background terms. This conclusion is correct for the specific case he considers, the $n=2$ levels of hydrogen, but follows from the very long radiative lifetime of the $2s$ state ($\gamma_{2s} \simeq 0$) and is not a general property of the anticrossing of levels of opposite parity. If neither of the two levels involved has $\gamma = 0$, there will be a contribution to the steady-state signal from term five of Eq. (1). Thus, Stark-induced anticrossing signals can be used to measure the Lamb shifts of the levels of hydrogen with $n > 2$.

Recently, Leventhal,[17] using electron-bombardment excitation and monitoring of the Lyman α line, observed a signal associated with the anticrossing of an s and p level of the $n=2$ term of hydrogen. This may seem surprising in view of the comments in the preceding paragraph. However, Leventhal's experiment was performed in a magnetic field of approximately 2300 G. For this field strength the lifetime of the $2s$ level involved is reduced to about 10^{-5} sec. by the coupling to distant p levels via the electric field seen by the atom as a result of its motion in the magnetic field. While Eq. (1) was derived for the case of optical excitation, it can easily be modified to give the form of the signal to be expected in Leventhal's experiment. Identifying state a

[12] A. Abragam and J. H. Van Vleck, Phys. Rev. **92**, 1448 (1953).
[13] J. P. van der Ziel and N. Bloembergen, Phys. Rev. **138**, A1287 (1965).
[14] R. T. Robiscoe, Phys. Rev. **138**, A22 (1965).
[15] E. B. Aleksandrov, Opt. Spectr. (USSR) **16**, 209 (1964) [English transl.: Opt. i Spectroskopiya **16**, 377 (1964)].
[16] B. Budick, S. Marcus, and R. Novick, Phys. Rev. **140**, A1041 (1965).
[17] M. Leventhal, Phys. Letters **20**, 625 (1966).

of Eq. (1) with the s state and b with the p state, we replace $\sum_m|f_{am}|^2$ and $\sum_m|f_{bm}|^2$ by r_s and r_p, the rates at which atoms are excited to these states by electron bombardment. Since there is no coherence in the excitation to or decay from these states, terms three, four, six, seven, and eight of Eq. (1) vanish. In addition to the nonresonant background signal from terms one and two, we have

$$S=\frac{-|2V|^2\gamma_s[(r_s/\gamma_s)-(r_p/\gamma_p)][(1/\gamma_s)\sum_{m'}(|g_{m's}|^2)-(1/\gamma_p)\sum_{m'}(|g_{m'p}|^2)]}{\gamma_s\gamma_p+|2V|^2+(4\gamma_s/\gamma_p)\Delta^2}$$

where we have replaced $\bar{\gamma}=\frac{1}{2}(\gamma_s+\gamma_p)$ by $\frac{1}{2}\gamma_p$, since $\gamma_s\ll\gamma_p$. The fullwidth at half maximum of this signal is

$$\Delta_{1/2}=\gamma_p(1+|2V|^2/\gamma_s\gamma_p)^{1/2}.$$

Leventhal's value of 14 G for the peak-to-peak derivative width of his signal corresponds to a $\Delta_{1/2}$ very nearly equal to γ_p, indicating that $\gamma_s\gamma_p\gg|2V|^2$.

Lamb and Sanders,[18] in connection with their investigation of the $n=3$ term of hydrogen, obtained an expression for the resonance signal when atoms are excited by electron bombardment and states of opposite parity are coupled by an rf electric field. Their result [Eq. (6) of Ref. 18] is essentially identical to term five of Eq. (1), if the interpretations of some of the factors of this term are appropriately altered. This demonstrates again the previously mentioned close kinship of anticrossing and double resonance signals.

Finally, we note that in principle all level crossings are really anticrossings, since all states of an atom are coupled to all other states in some order of perturbation by stray electric fields. However, if the matrix element V coupling the states a and b is small compared to γ_a and γ_b, the signal in the region of the crossing is indistinguishable from that for $V=0$. A case in point occurs for the low-field fine structure crossing in the $2\,^2P$ term of Li^7, where off-diagonal matrix elements of the electric quadrupole hyperfine interaction couple the state $J=\frac{3}{2}$, $m_J=-\frac{3}{2}$, $m_I=\frac{3}{2}$ to the state $\frac{1}{2}$, $\frac{1}{2}$, $-\frac{1}{2}$ and the state $\frac{3}{2}$, $-\frac{3}{2}$, $\frac{1}{2}$ to the state $\frac{1}{2}$, $\frac{1}{2}$, $-\frac{3}{2}$. Thus, with the Polaroid axes aligned parallel to **H** to eliminate the normal crossing signal, one might hope to see two well resolved signals from these two anticrossings. Our failure to observe such signals above the noise level is not surprising, since the ratio $|V|/\gamma$ is only about 4×10^{-2} compared to a value of 4.3 for the anticrossing that was observed in Li^7.

ACKNOWLEDGMENTS

We are indebted to L. L. Foldy for pointing out to us the role played by the magnetic hyperfine interaction in the anticrossing signals observed in lithium and for many illuminating conversations related to the theory of anticrossing.

[18] W. E. Lamb, Jr., and T. M. Sanders, Jr., Phys. Rev. **119**, 1901 (1960).

APPENDIX A: DERIVATION OF ANTICROSSING SIGNAL

Series[8] has considered the resonance-fluorescence signal from the anticrossing of two states $|a\rangle$ and $|b\rangle$ for the special case where one of the states does not radiate ($\gamma_a=0$). He finds that for this limiting situation the steady-state signal is independent of the separation between the two levels and of the coupling between the two states. We shall treat the more general case of arbitrary γ_a and γ_b using the same approach as Series, but with slight changes in notation.

The states $|a\rangle$ and $|b\rangle$ are eigenstates of the Hamiltonian $\mathcal{H}_0$ with eigenvalues $\hbar\omega_a$ and $\hbar\omega_b$. Radiative decay is handled by introducing a damping Hamiltonian $\mathcal{H}_D$ whose matrix is diagonal, with elements $-\frac{1}{2}i\hbar\Gamma_a$ for $|a\rangle$ and $-\frac{1}{2}i\hbar\Gamma_b$ for $|b\rangle$ ($\Gamma_a=1/\tau_a$, where τ_a is the mean lifetime of state $|a\rangle$). The states $|a\rangle$ and $|b\rangle$ are coupled by the time-independent perturbation $\mathcal{H}'$.

The wave function of the atom at time t is found by solving the Schrödinger equation

$$i\hbar(\partial|t\rangle/\partial t)=(\mathcal{H}_0+\mathcal{H}_D+\mathcal{H}')|t\rangle.$$

Assuming a solution of the form

$$|t\rangle=a(t)\exp(-i\omega_a t)|a\rangle+b(t)\exp(-i\omega_b t)|b\rangle$$

and using the orthogonality of $|a\rangle$ and $|b\rangle$, we obtain

$$\begin{aligned}i\dot{a}&=-\tfrac{1}{2}ia\Gamma_a+2\pi Vb\exp(i\omega t),\\ i\dot{b}&=-\tfrac{1}{2}ib\Gamma_b+2\pi V^*a\exp(-i\omega t),\end{aligned}\tag{A1}$$

where $\omega=\omega_a-\omega_b$ and $V=\langle a|\mathcal{H}'|b\rangle/2\pi\hbar$. Substituting the trial solutions

$$\begin{aligned}a&=\sum_{n=1}^{2}A_n\exp(\alpha_n t+i\omega_a t),\\ b&=\sum_{n=1}^{2}B_n\exp(\alpha_n t+i\omega_b t),\end{aligned}\tag{A2}$$

into Eq. (A1) yields

$$B_n=i(\alpha_n+i\omega_a+\tfrac{1}{2}\Gamma_a)(A_n/2\pi V),$$

and

$$\alpha_{1,2}=-[\tfrac{1}{4}(\Gamma_a+\Gamma_b)+\tfrac{1}{2}i(\omega_a+\omega_b)]\pm\{[(\Gamma_a-\Gamma_b)/4+\tfrac{1}{2}i\omega]^2-|2\pi V|^2\}^{1/2},$$

where the plus sign in front of the square root goes with α_1. Setting $t=0$ in Eq. (A2) and taking $a(0)=f_{am}$ and

$b(0)=f_{bm}$, gives

$$A_1=-[(\alpha_2+i\omega_a+\tfrac{1}{2}\Gamma_a)f_{am}+i2\pi Vf_{bm}]/(\alpha_1-\alpha_2),$$
$$A_2=[(\alpha_1+i\omega_a+\tfrac{1}{2}\Gamma_a)f_{am}+i2\pi Vf_{bm}]/(\alpha_1-\alpha_2).$$

$f_{am}=\langle a|\mathbf{f}\cdot\mathbf{r}|m\rangle$ is the electric dipole matrix element for excitation from the ground state $|m\rangle$ to state $|a\rangle$ by photons of polarization **f**.

The intensity of the scattered light reaching the detector is proportional to the square of the electric dipole matrix element $\langle m'|\mathbf{g}\cdot\mathbf{r}|t\rangle$ for spontaneous decay to the final state $|m'\rangle$ via photons of polarization **g**. Thus, the detected signal is proportional to

$$|a(t)g_{m'a}\exp(-i\omega_a t)+b(t)g_{m'b}\exp(-i\omega_b t)|^2.$$

The preceding discussion assumes that the atom is excited at $t=0$. To find the steady-state signal from a collection of atoms excited at a uniform rate, we replace t in the above expression for $|\langle m'|\mathbf{g}\cdot\mathbf{r}|t\rangle|^2$ by $t-t_0$ and integrate over t_0 from $-\infty$ to t. This yields

$$\begin{aligned}S=&-|g_{m'a}|^2[|A_1|^2/(\alpha_1+\alpha_1^*)+|A_2|^2/(\alpha_2+\alpha_2^*)+A_1A_2^*/(\alpha_1+\alpha_2^*)+A_1^*A_2/(\alpha_1^*+\alpha_2)]\\&-|g_{m'b}|^2[|B_1|^2/(\alpha_1+\alpha_1^*)+|B_2|^2/(\alpha_2+\alpha_2^*)+B_1B_2^*/(\alpha_1+\alpha_2^*)+B_1^*B_2/(\alpha_1^*+\alpha_2)]\\&-g_{m'a}g_{m'b}^*[A_1B_1^*/(\alpha_1+\alpha_1^*)+A_2B_2^*/(\alpha_2+\alpha_2^*)+A_1B_2^*/(\alpha_1+\alpha_2^*)+A_2B_1^*(\alpha_1^*+\alpha_2)]\\&-g_{m'a}^*g_{m'b}[A_1^*B_1/(\alpha_1+\alpha_1^*)+A_2^*B_2/(\alpha_2+\alpha_2^*)+A_1^*B_2/(\alpha_1^*+\alpha_2)+A_2^*B_1/(\alpha_1+\alpha_2^*)].\end{aligned}\quad\text{(A3)}$$

We assume that all factors having to do with the intensity and spectral distribution of the resonance lamp, the spectral sensitivity of the detector, polarizations of incident and scattered light, experimental geometry, etc., are contained in the matrix elements f_{am}, $g_{m'a}$, etc. Equation (A3), after much straightforward but tedious algebraic manipulation, yields the form for the signal given by Eq. (1) of Sec. II. In Eq. (1) we have summed over all possible values of the initial state m and final state m', and have replaced ω by $2\pi\Delta$ and Γ by $2\pi\gamma$ to convert from units of angular frequency to those of frequency.

APPENDIX B: ANALYSIS OF OVERLAPPING ANTICROSSING SIGNALS

The off-diagonal matrix element V, responsible for the anticrossing phenomenon, can be determined from the peak-to-peak derivative width of the anticrossing signal, provided τ, the lifetime of the excited state, is known. Since the anticrossing signals observed in the $2\,^2P$ term of Li are composite curves made up of closely spaced hyperfine components, we must have some way of deducing the width of an individual component from the observed width of the composite curve.

Let us consider in detail the calculation for Li^6. Here, the anticrossing signal is proportional to $[1+(\omega-\omega_0/2)^2]^{-1}+[1+(\omega+\omega_0/2)^2]^{-1}$, where ω_0 is the dimensionless spacing of the two hyperfine components of the anticrossing. Since $\omega_0<1$, this expression can be binomially expanded in powers of $\omega_0^2/(1+\omega^2)$ (odd powers of ω_0 obviously cancel in the expansion). Neglecting terms of the order ω_0^4 and higher, and solving for the derivative extrema in the usual manner, we obtain

$$1-3\omega^2-\tfrac{3}{2}\omega_0^2(1-10\omega^2+5\omega^4)(1+\omega^2)^{-2}=0.$$

Since the third term in the above equation is a small correction, it is safe to substitute for ω^2 in this term the value $\frac{1}{3}$ obtained by setting $\omega_0=0$. The final result is

$$P=P'-\omega_0^2/P',$$

where P is the peak-to-peak derivative width of an individual hyperfine component and P' is the observed peak-to-peak derivative width of the composite signal. ω_0 is calculable from a knowledge of $\alpha\langle 1/r^3\rangle$ and ξ. For the widths and spacings of this experiment, the error introduced in the above expression for P (and the corresponding expression for Li^7) due to neglecting the higher order terms in ω_0 is certainly less than 1%.

A similar calculation for the Li^7 anticrossing signal, which has three overlapping components, gives

$$P=P'-(8/3)\omega_0^2/P',$$

where ω_0 is the spacing between adjacent components.